ACS APPLIED MATERIALS & INTERFACES

Research Article

www.acsami.org

Photoinduced Charge Transfer in Donor–Acceptor (DA) Copolymer: Fullerene Bis-adduct Polymer Solar Cells

Tae Eui Kang,[†] Han-Hee Cho,[†] Chul-Hee Cho,[†] Ki-Hyun Kim,[†] Hyunbum Kang,[†] Myounghee Lee,[‡] Sunae Lee,[‡] BongSoo Kim,[§] Chan Im,[‡] and Bumjoon J. Kim*[,†]

[†]Department of Chemical and Biomolecular Engineering, Korea Advanced Institute of Science and Technology (KAIST), Daejeon 305-701, Korea

[‡]Konkuk University–Fraunhofer ISE Next Generation Solar Cell Research Center, 120 Neungdong-ro, Gwangjin-gu, Seoul 143-701, Korea

[§]Photo-electronic Hybrids Research Center, Korea Institute of Science and Technology (KIST), Seoul 136-791, Korea

Supporting Information

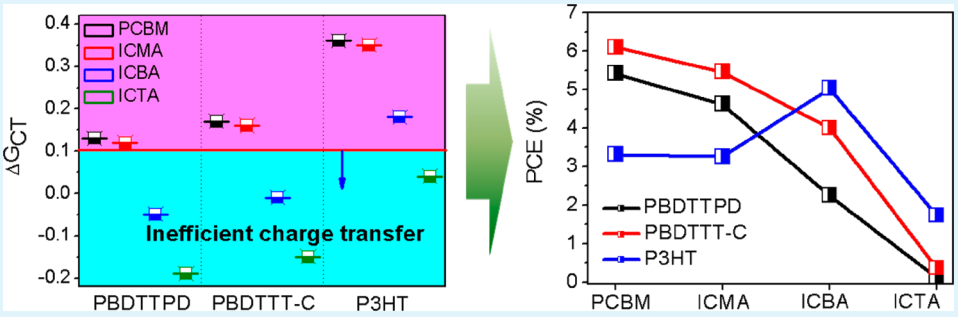

ABSTRACT: Polymer solar cells (PSCs) consisting of fullerene bis-adduct and poly(3-hexylthiophene) (P3HT) blends have shown higher efficiencies than P3HT:phenyl C_{61}-butyric acid methyl ester (PCBM) devices, because of the high-lying lowest unoccupied molecular orbital (LUMO) level of the fullerene bis-adducts. In contrast, the use of fullerene bis-adducts in donor–acceptor (DA) copolymer systems typically causes a decrease in the device's performance due to the decreased short-circuit current (J_{SC}) and the fill factor (FF). However, the reason for such poor performance in DA copolymer:fullerene bis-adduct blends is not fully understood. In this work, bulk-heterojunction (BHJ)-type PSCs composed of three different electron donors with four different electron acceptors were chosen and compared. The three electron donors were (1) poly[(4,8-bis-(2-ethylhexyloxy)benzo[1,2-*b*:4,5-*b*′]dithiophene)-2,6-diyl-*alt*-(5-octylthieno[3,4-*c*]pyrrole-4,6-dione)-1,3-diyl] (PBDTTPD), (2) poly[(4,8-bis-(2-ethylhexyloxy)benzo[1,2-*b*:4,5-*b*′]dithiophene)-2,6-diyl-*alt*-(4-(2-ethylhexanoyl)-thieno[3,4-*b*]thiophene)-2,6-diyl] (PBDTTT-C), and (3) P3HT polymers. The four electron acceptors were (1) PCBM, (2) indene-C_{60} monoadduct (ICMA), (3) indene-C_{60} bis-adduct (ICBA), and (4) indene-C_{60} tris-adduct (ICTA). To understand the difference in the performance of BHJ-type PSCs for the three different polymers in terms of the choice of fullerene acceptor, the structural, optical, and electrical properties of the blends were measured by the external quantum efficiency (EQE), photoluminescence, grazing incidence X-ray scattering, and transient absorption spectroscopy. We observed that while the molecular packing and optical properties cannot be the main reasons for the dramatic decrease in the PCE of the DA copolymers and ICBA, the value of the driving force for charge transfer (ΔG_{CT}) is a key parameter for determining the change in J_{SC} and device efficiency in the DA copolymer- and P3HT-based PSCs in terms of fullerene acceptor. The low EQE and J_{SC} in PBDTTPD and PBDTTT-C blended with ICBA and ICTA were attributed to an insufficient ΔG_{CT} due to the higher LUMO levels of the fullerene multiadducts. Quantitative information on the efficiency of the charge transfer was obtained by comparing the polaron yield, lifetime, and exciton dissociation probability in the DA copolymer:fullerene acceptor films.

KEYWORDS: *photoinduced charge transfer, driving force for charge transfer (ΔG_{CT}), donor–acceptor (DA) copolymer, fullerene bis-adduct, polymer solar cell*

INTRODUCTION

Bulk-heterojunction (BHJ)-type polymer solar cells (PSCs) have attracted significant attention as a potential alternative energy source due to their lightweight, easy solution-processability, flexibility, and low cost of fabrication.[1,2] However, a power conversion efficiency (PCE) of greater than 10% is a prerequisite for their commercialization.[3] Recently, donor–acceptor (DA) copolymers have been studied intensively with the aim of matching

Received: October 27, 2012
Accepted: January 4, 2013
Published: January 4, 2013

   dx.doi.org/10.1021/am302479u | *ACS Appl. Mater. Interfaces* 2013, 5, 861–868

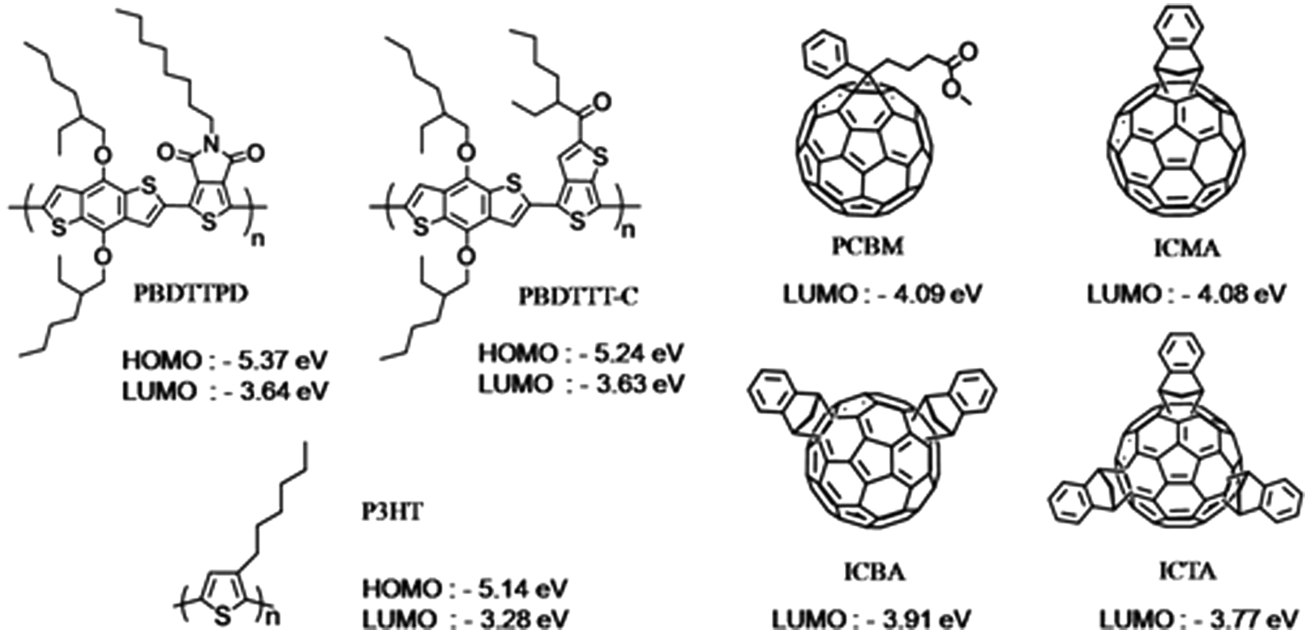

Figure 1. Chemical structures of the electron-donor and electron-acceptor materials used in this study: HOMO and LUMO represent E_{HOMO}^{OPT} and E_{LUMO}^{OPT}, respectively (Table 2).

a greater part of the solar spectrum and thus harvesting the maximum photon flux, thereby producing high efficiencies of greater than 6−8%.[4−11] The high J_{SC} in the DA copolymer-based PSCs must be combined with high open-circuit voltage (V_{OC}) to further increase their performance.

To address this issue, researchers have designed and synthesized a number of fullerene derivatives with high lowest unoccupied molecular orbital (LUMO) levels for use as electron acceptors to increase the V_{OC} in PSCs.[12−20] In particular, by replacing phenyl C_{61}-butyric acid methyl ester (PCBM) with fullerene bis-adduct that has a high LUMO level, BHJ-type PSCs based on poly(3-hexylthiophene) (P3HT) have shown significantly enhanced PCE values due to their high V_{OC} (>0.8 V).[15,17,21,22] However, most BHJ-type PSCs, consisting of DA copolymer and fullerene bis-adduct, showed lower PCE values than PSCs made of DA copolymer and fullerene monoadduct (i.e., PCBM).[12,23−26] The fullerene multiadducts in the blend induced changes in charge mobility, optical properties, and miscibility with electron-donating polymers, resulting in changes in the blend's morphology.[27,28] At the same time, they typically increased the value of V_{OC} due to the high LUMO level but decreased the driving force (ΔG_{CT}) for charge transfer between the donor and the acceptor. In particular, the charge transfer (CT) state formed via the transfer of the photoinduced charge between the electron donor and the electron acceptor is dependent on the LUMO level of the fullerenes. Because the energy of the CT state (E_{CT}) affects the V_{OC} as well as the J_{SC},[29−31] the optimization of E_{CT} and ΔG_{CT} is a critical requirement for the design of DA copolymer:fullerene bis-adduct PSCs with high J_{SC} and V_{OC} values.

To investigate the effect of fullerene bis- and tris-adducts on the performance of BHJ-type PSCs, three different polymers, i.e., (1) poly[(4,8-bis-(2-ethylhexyloxyl)benzo[1,2-*b*:4,5-*b*′]dithiophene)-2,6-diyl-*alt*-(5-octylthieno[3,4-*c*]pyrrole-4,6-dione)-1,3-diyl] (PBDTTPD),[8,32,33] (2) poly[(4,8-bis-(2-ethylhexyloxy)-benzo[1,2-*b*:4,5-*b*′]dithiophene)-2,6-diyl-*alt*-(4-(2-ethylhexanoyl)-thieno[3,4-*b*]thiophene)-2,6-diyl] (PBDTTT-C),[34,35] and (3) P3HT were blended with four different acceptors that possessed different LUMO levels, i.e., (1) PCBM, (2) indene-C_{60} monoadduct (ICMA), (3) indene-C_{60} bis-adduct (ICBA), and (4) indene-C_{60} tris-adduct (ICTA) (Figure 1). The performances of the DA copolymer-based (PBDTTPD and PBDTTT-C) BHJ-type PSCs were compared with the performances of the P3HT-based devices. While the PCE of P3HT:ICBA devices exhibited higher performance than the P3HT:PCBM and P3HT:ICMA devices, the PCEs of PBDTTPD:ICBA and PBDTTT-C:ICBA were lower than those with fullerene monoadduct. To understand the differences in the behavior of DA copolymers and P3HT, the EQE, photoluminescence (PL), and transient absorption (TA) spectroscopy were measured and compared. The ΔG_{CT} value can explain the change in J_{SC} and PCE in both the DA copolymer and the P3HT-based PSCs, which agrees with previous findings that the critical value of 0.1 eV for ΔG_{CT} is required to obtain efficient photoinduced charge transfer and high J_{SC} values.[24,36] Our measurements of the polaron yield and lifetime and the probability of exciton dissociation can provide a quantitative understanding of the performance of BHJ-type PSCs for the three different polymers in terms of the choice of the fullerene acceptor.

RESULTS AND DISCUSSION

BHJ-type PSCs with the structure of indium tin oxide (ITO)/poly(3,4-ethylenedioxythiophene):poly(styrenesulfonate) (PEDOT:PSS)/active layer/LiF/Al were fabricated, and their performances were measured under AM 1.5 G simulated solar illumination (Figure 2). In the active layer, PBDTTPD, PBDTTT-C, and P3HT were used as electron donors, and PCBM, ICMA, ICBA, and ICTA were used as electron acceptors. Table 1 summarizes the characteristics of the PSC devices at optimized conditions. High-boiling-point additives (1,8-diiodooctane) were used for the PBDTTPD and PBDTTT-C based devices, while thermal annealing was applied for the P3HT-based PSCs to optimize their performance. The P3HT:ICBA device (PCE = 5.03%) outperformed the P3HT:PCBM (PCE = 3.31%) and P3HT:ICMA (PCE = 3.26%) devices because of an increase in

dx.doi.org/10.1021/am302479u | ACS Appl. Mater. Interfaces 2013, 5, 861−868

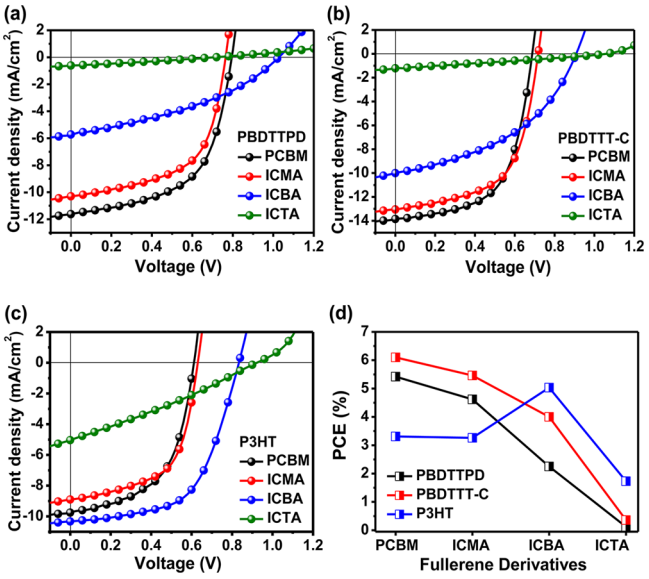

Figure 2. Current–voltage (J–V) characteristics of BHJ-type PSCs of PCBM, ICMA, ICBA, and ICTA with (a) PBDTTPD, (b) PBDTTT-C, and (c) P3HT under AM 1.5 G simulated solar illumination (100 mW/cm^2). (d) Variations of their PCE values.

V_{OC}. On the other hand, the P3HT:ICTA device had a low PCE value of 1.35%. Despite its high V_{OC} of 0.92 V, the device suffered from the low J_{SC} and fill factor (FF) values that were caused by the low electron mobility of ICTA.[18] The PSC devices of the PBDTTPD and PBDTTT-C blends with fullerene bis-adduct exhibited a different trend than the devices based on P3HT. Both the PBDTTPD and PBDTTT-C based devices exhibited their highest performance when fullerene monoadduct was used as the electron acceptor. For example, PBDTTPD:PCBM and PBDTTT-C:PCBM devices had PCE values of 5.42 and 5.91%, respectively. When the fullerene bis-adduct of ICBA was used as the electron acceptor, the PBDTTPD and PBDTTT-C based PSCs exhibited reduced performances of 2.25 and 4.00%, respectively. Although V_{OC} increased (from 0.77 to 1.06 V for PBDTTPD and from 0.72 to 0.91 V for PBDTTT-C), both the J_{SC} and the FF values of the ICBA devices decreased dramatically compared to fullerene monoadduct-based devices. In addition, the use of ICTA in the PBDTTPD and PBDTTT-C systems caused further decreases in performance, including J_{SC} and FF. Although the use of ICBA and ICTA caused decreases in both the PBDTTPD and PBDTTT-C PSCs, their effect on the trend of V_{OC} and PCE was different in the two systems. For example, a linear increase of V_{OC} was observed for the PBDTTT-C blend films in the order ICMA < ICBA < ICTA (0.72, 0.91, and 1.06 V, respectively), which was similar to the trend for the P3HT-based devices, i.e., 0.64, 0.83, and 0.92 V, respectively. This result was expected due to the differences in the LUMO levels of ICMA, ICBA, and ICTA. In contrast, the V_{OC} value of the PBDTTPD:ICTA blend (0.71 V) was reduced dramatically compared to the V_{OC} value of the PBDTTPD:ICBA device (1.06 V). In addition, the degree of reduction in J_{SC} that occurred by replacing PCBM with ICBA was significantly different between the PBDTTPD and PBDTTT-C based devices. While the decrease in J_{SC} from PBDTTT-C:PCBM to PBDTTT-C:ICBA was only 28%, the J_{SC} value decreased by 51% for the PBDTTPD devices.

The light absorption in the active layer was one of the main factors that determine the J_{SC} values in solar cells. The UV–vis absorption spectra of the different PBDTTPD, PBDTTT-C, and P3HT films blended with PCBM, ICMA, ICBA, and ICTA were measured to determine their optical properties and the change in the packing structure of PBDTTPD, PBDTTT-C, and P3HT in the blend films (Figure 3a, c, and e). All of the blend samples were prepared by spin-coating on glass substrates under optimized conditions. In all of the PBDTTPD-blended films, the optical absorption spectra displayed three maxima in the range of 300–700 nm. Although the PBDTTPD films blended with ICBA and ICTA exhibited slightly reduced peak intensities, there was no difference in the location of the peaks. In particular, the location of the vibronic peak (~623 nm), which was indicative of the π–π stacking of the polymer backbone, was unchanged when different electron acceptors were used. This result indicated that the packing structure of PBDTTPD blends was not influenced by the presence of the fullerene multiadducts. This consistent packing structure was confirmed by the results from the grazing incidence X-ray scattering (GIXS) measurements (Supporting Information Figure S1). And the optical spectra of PBDTTT-C blends in terms of fullerene acceptors exhibited similar trend as those of PBDTTPD blends, showing no change in the location of the peaks but slightly reduced intensities with the use of the fullerene multiadducts (Figure 3c). In the case of the P3HT blend, the peak intensities from 450 to 650 nm were reduced slightly when ICBA and ICTA were used (Figure 3e). Therefore, we note that the molecular packing and optical properties cannot be the primary reasons for the dramatic decrease in the PCE of the DA copolymers and ICBA.

Table 1. Characteristics of BHJ-type PSC Devices (AM 1.5 G Illumination Conditions)

polymer:acceptor		thickness (nm)	V_{OC} (V)	J_{SC} (mA·cm^{-2})	FF	PCE$_{max}$ (PCE$_{avg}$) (%)
PBDTTPD	PCBM	105	0.80	11.80	0.57	5.42 (5.39)
	ICMA	100	0.77	10.40	0.57	4.62 (4.55)
	ICBA	110	1.06	5.75	0.37	2.25 (2.20)
	ICTA	110	0.71	0.60	0.28	0.12 (0.10)
PBDTTT-C	PCBM	80	0.70	13.90	0.60	5.91 (5.87)
	ICMA	85	0.72	12.90	0.59	5.46 (5.40)
	ICBA	80	0.91	10.00	0.44	4.00 (3.92)
	ICTA	90	1.06	1.21	0.28	0.36 (0.34)
P3HT	PCBM	120	0.62	9.74	0.55	3.31 (3.24)
	ICMA	105	0.64	8.26	0.57	3.26 (3.13)
	ICBA	90	0.83	10.50	0.58	5.03 (4.98)
	ICTA	100	0.92	5.08	0.30	1.35 (1.28)

dx.doi.org/10.1021/am302479u | ACS Appl. Mater. Interfaces 2013, 5, 861–868

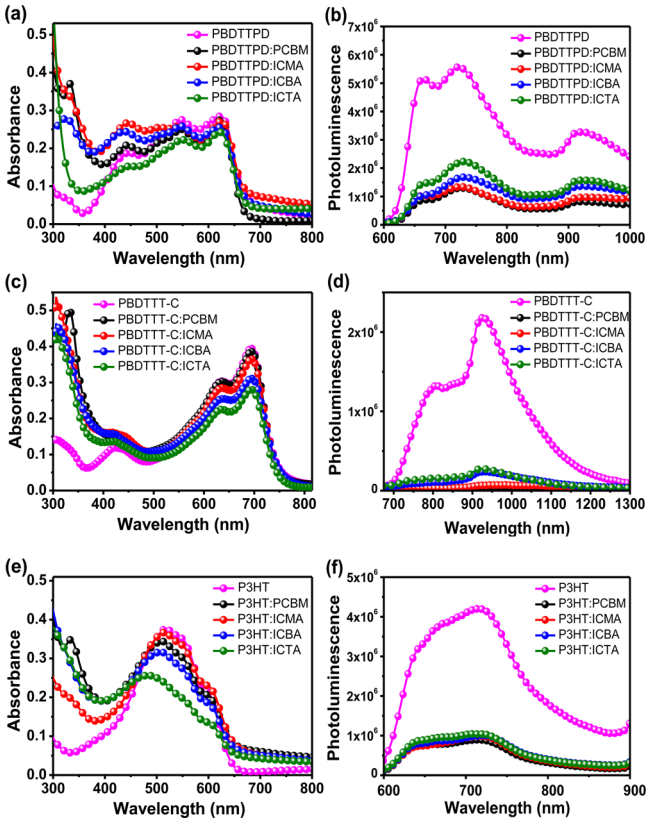

Figure 3. UV–vis absorption (a, c, and e) and static PL spectra (b, d, and f) for PBDTTPD, PBDTTT-C, and P3HT, respectively, blended with the PCBM (black), ICMA (red), ICBA (blue), and ICTA (green) films. The blend films were prepared under optimized conditions for device fabrication. The pristine polymer films (pink) were measured as controls.

The PL of the PBDTTPD, PBDTTT-C, and P3HT samples blended with PCBM, ICMA, ICBA, and ICTA were measured with excitation wavelengths of 620, 520, and 460 nm, respectively (Figure 3b, d, and f). To compare the degree of PL quenching, the fluorescence spectra of pristine PBDTTPD, PBDTTT-C, and P3HT films were measured as controls. In the P3HT films, the degree of PL quenching for the four different acceptors was almost the same (Figure 3f). As shown in Figure 3b, the PL quenching of PBDTTPD blended with four acceptors decreased in the order PCBM (ICMA) > ICBA > ICTA, but the changes in the PL quenching were not significant. For example, while the PL intensity of the PBDTTPD:PCBM blend was quenched by ~77% compared to the PL intensity of pristine PBDTTPD, the intensities of the PBDTTPD:ICBA and PBDTTPD:ICTA films were quenched by ~70% and ~60%, respectively. In the case of PBDTTT-C blends, the PL quenching efficiencies of PBDTTT-C blended with ICBA and ICTA were 89% and 87%, respectively, smaller than those with PCBM (98%) and ICMA (97%).

Figure 4 presents the EQE curves to evaluate the photoresponse of the PBDTTPD, PBDTTT-C, and P3HT film blends. The PBDTTPD films blended with ICBA and ICTA had EQE values less than 30% and 5%, respectively, in the wavelength range from 400 to 700 nm, which is in stark contrast to the EQE values of the PBDTTPD:fullerene monoadduct films. Similarly, the PBDTTT-C films blended with ICBA and ICTA exhibited EQE values less than 45% and 5%, respectively, which is significantly lower than the EQE value of the PBDTTT-C:PCBM film (Figure 4b). In contrast, the EQE of the P3HT films blended with PCBM, ICMA, and ICBA had responses greater than 50%, and only ICTA was below 35% (Figure 4c). The measured J_{SC} values for all of the PSC devices were well matched with integrated values obtained from the EQE spectrum within an error of 3%. The combined results of the UV–vis absorption, PL quenching, and EQE measurements suggested that the difference in the electrical properties, such as the charge transfer and transport between PBDTTPD (or PBDTTT-C):fullerene monoadduct and PBDTTPD (or PBDTTT-C):ICBA films, could be the main reason for the dramatic change in the J_{SC} and PCE values. To examine this possibility, the hole and electron mobilities of the PBDTTPD blend films with different fullerene acceptors were measured and compared (Supporting Information Figure S3). The hole-only device was fabricated using the ITO/PEDOT:PSS/blend/Au structure, while the electron-only device was fabricated using the ITO/CS_2CO_3/blend/LiF/Al structure. The changes in both the hole and electron mobilities from the PBDTTPD:fullerene monoadduct to PBDTTPD:ICBA were not significant. In addition, the PBDTTPD:ICBA film retained a good balance between the hole and electron mobilities, indicating that the charge transport might not be a major reason for the low EQE and J_{SC} values in the PBDTTPD:ICBA film. Therefore, the lower Jsc and EQE values of PBDTTPD:ICBA and PBDTTT-C:ICBA compared to those of P3HT:ICBA could be due to the inefficient charge transfer, which will be discussed in the section below.

The CT state, an intermediate state between the exciton and the separated charges, plays a crucial role in the process of the photoinduced charge transfer between the electron donor and the electron acceptor (Figure 5a).[31,37] In this process, ΔG_{CT}, which is equal to $E_g - E_{CT}$, is a critical parameter in determining the charge transfer from the lowest singlet excited state to the CT state.[36] E_g represents the optical band gap, defined as the lowest first singlet state energy of either the donor or the acceptor, while E_{CT} represents the energy of the CT state. In this regard,

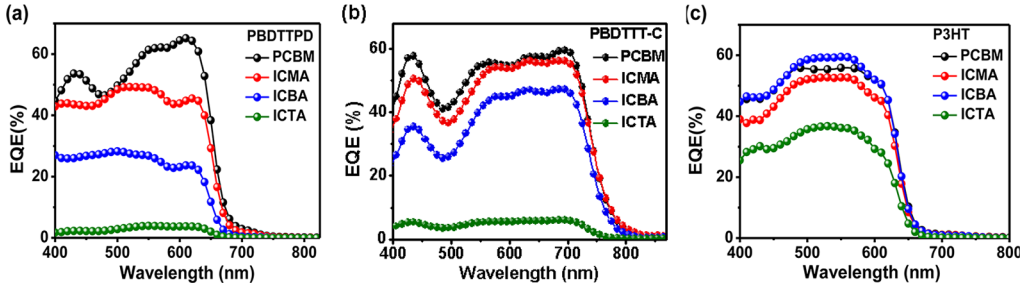

Figure 4. EQE curves for (a) PBDTTPD, (b) PBDTTT-C, and (c) P3HT blended with PCBM (black), ICMA (red), ICBA (blue), and ICTA (green) films.

dx.doi.org/10.1021/am302479u | ACS Appl. Mater. Interfaces 2013, 5, 861–868

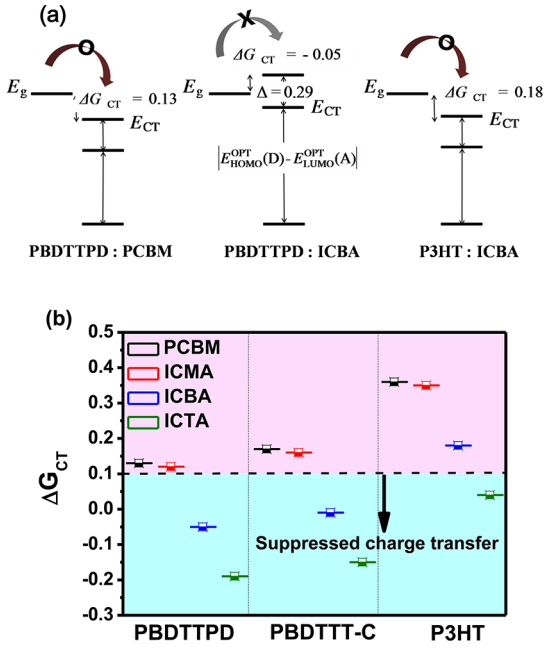

Figure 5. (a) Energy diagram for photoinduced charge transfer in polymer:fullerene blend films. Note that E_g represents the lowest energies of the optical band gap E_g(Donor) or E_g(Acceptor) and ΔG_{CT} indicates the driving force for charge transfer. (b) Diagram summarizes the ΔG_{CT} values for the PBDTTPD, PBDTTT-C, and P3HT blends with different fullerene acceptors.

we calculated the values of ΔG_{CT} for the PBDTTPD, PBDTTT-C, and P3HT systems blended with the four different acceptors (PCBM, ICMA, ICBA, and ICTA) following the procedure reported by Janssen et al.[36] First, to compensate for the difference between the electrochemical and optical band gaps, the effective band gaps (E^{OPT}_{LUMO} and E^{OPT}_{HOMO}) were calculated using eqs 1 and 2, where E^{sol}_{cv} can be measured by cyclic voltammetry (CV) in solution, and E_g can be measured in the film by UV−vis spectroscopy. The absolute energy level of −4.80 eV with respect to the vacuum level was used for the redox potential of ferrocene/ferrocenium (Fc/Fc^+).[38,39] The optical band gap values of the fullerene acceptors (PCBM, ICMA, ICBA, and ICTA) were measured to be 1.70 eV, which agrees well with the reported values.[24,36] From the E^{OPT}_{LUMO} and E^{OPT}_{HOMO} values, the values of E_{CT} and ΔG_{CT} were estimated and summarized in Tables 2 and 3.

$$E^{OPT}_{HOMO} = -4.80\ \text{eV} - eE_{ox} + \frac{1}{2}(E^{sol}_{cv} - E_g) \quad (1)$$

$$E^{OPT}_{LUMO} = -4.80\ \text{eV} - eE_{red} - \frac{1}{2}(E^{sol}_{cv} - E_g) \quad (2)$$

In Table 3, the E_{CT} values for the PBDTTPD, PBDTTT-C, and P3HT blend films increased gradually in the order of PCBM (ICMA), ICBA, and ICTA because of the difference in their

Table 3. Values of E_{CT} and ΔG_{CT} in the PBDTTPD, PBDTTT-C, and P3HT Blends with Different Fullerene Acceptors

blend						
donor	acceptor	E_{red}(A)	E^{OPT}_{LUMO} (A)	E^{OPT}_{HOMO} (D)−E^{OPT}_{LUMO}(A)	E_{CT} [a]	ΔG_{CT} [b]
PBDTTPD	PCBM	−0.95	−4.09	−1.28	1.57	+0.13
	ICMA	−0.96	−4.08	−1.29	1.58	+0.12
	ICBA	−1.13	−3.91	−1.46	1.75	−0.05
	ICTA	−1.27	−3.77	−1.60	1.89	−0.19
PBDTTT-C	PCBM	−0.95	−4.09	−1.15	1.44	+0.17
	ICMA	−0.96	−4.08	−1.16	1.45	+0.16
	ICBA	−1.13	−3.91	−1.33	1.62	−0.01
	ICTA	−1.27	−3.77	−1.47	1.76	−0.15
P3HT	PCBM	−0.95	−4.09	−1.05	1.34	+0.36
	ICMA	−0.96	−4.08	−1.06	1.35	+0.35
	ICBA	−1.13	−3.91	−1.23	1.52	+0.18
	ICTA	−1.27	−3.77	−1.37	1.66	+0.04

[a]Values calculated by $E_{CT} = |E^{OPT}_{HOMO}(D) - E^{OPT}_{LUMO}(A)| + 0.29$ eV. [b]$\Delta G_{CT} = E_g - E_{CT}$ (ref 36).

LUMO levels. The values of E_{CT} in PBDTTPD:PCBM and PBDTTPD:ICBA were consistent with the results from the McGehee group,[25] who estimated the values based on the EQE and electroluminescence data. The increasing trend of E_{CT} matched well with the increasing trend of V_{OC} as shown in Tables 1 and 3. In general, the V_{OC} values of the PSCs for the blends of PBDTTPD, PBDTTT-C, and P3HT were lower than the E_{CT} values by ∼0.7 V due to radiative and nonradiative recombination.[29] The only exception was found for the PBDTTPD:ICTA blend film, which has the lowest ΔG_{CT} value among all of the samples.

While the high V_{OC} values in PBDTTPD and PBDTTT-C blended with ICBA were induced by their high E_{CT}, the high E_{CT} also caused a decrease in the ΔG_{CT} values. Table 3 shows that the P3HT blends with PCBM, ICMA, and ICBA have sufficient ΔG_{CT}, i.e., greater than +0.18 eV, whereas the ΔG_{CT} of P3HT:ICTA was 0.04 eV. In contrast to the P3HT blends, only the films of PBDTTPD and PBDTTT-C blended with PCBM and ICMA had ΔG_{CT} values greater than 0.10 eV, whereas PBDTTPD and PBDTTT-C blended with ICBA exhibited insufficient ΔG_{CT} values that resulted in limited charge transfer. Therefore, the ΔG_{CT} values as a function of the fullerenes can explain the trends in the device's performance, especially in terms of J_{SC}. Our results agree excellent with the previous findings,[36] showing that the ΔG_{CT} value of 0.1 eV is required to ensure efficient photoinduced charge transfer and high J_{SC} values. In addition, the ΔG_{CT} value for PBDTTPD:ICBA (−0.05 eV) was less than the ΔG_{CT} value for PBDTTT-C:ICBA (−0.01 eV). This difference facilitated the understanding of the differences in the J_{SC} and EQE values of the PSCs. While the decrease in J_{SC} from PBDTTT-C:PCBM to PBDTTT-C:ICBA was 28%, the J_{SC} value decreased by 51% for the

Table 2. Calculation of E^{OPT}_{LUMO} and E^{OPT}_{HOMO} Values of the Polymers from their E_g and E^{sol}_{cv} Values

polymer	E_g (eV)[a]	E^{sol}_{cv} (eV)[b]	E_{ox}	E_{red}	$(E^{sol}_{cv}-E_g)/2$	E^{OPT}_{HOMO} [c]	E^{OPT}_{LUMO} [c]
PBDTTPD	1.74	1.83	0.62	−1.21	0.05	−5.37	−3.64
PBDTTT-C	1.61	1.67	0.47	−1.20	0.03	−5.24	−3.63
P3HT	1.86	1.92[d]	0.37	−1.55	0.03	−5.14	−3.28

[a]Optical energy gap estimated from the absorption edge of the as-cast thin film. [b]Band gap obtained from CV measurements. [c]Calculated values from eqs 1 and 2. [d]The value from ref 36.

dx.doi.org/10.1021/am302479u | ACS Appl. Mater. Interfaces 2013, 5, 861−868

PBDTTPD devices. And because the CT states of PBDTTPD:ICTA and PBDTTT-C:ICTA were above even the lowest singlet excited state, the inefficient charge transfer and extremely low J_{SC} for PBDTTPD:ICTA and PBDTTT-C:ICTA were to be expected.

A deeper insight into the effect of fullerene multiadducts on the charge transfer between the donor and the acceptor materials can be obtained by transient absorption (TA) spectroscopy. Quantitative information on the efficiency of the charge transfer in the DA copolymer:fullerene systems can be obtained from the population of polarons (polaron yield) in the CT state. TA spectroscopy was performed for the PBDTTPD and PBDTTT-C blend films with an excitation wavelength of 610 nm. These samples were prepared in optimized device conditions without electrode-on-glass substrates. The pristine polymer films of PBDTTPD and PBDTTT-C were prepared as the reference samples. It was found that the polarons in the PBDTTPD and PBDTTT-C blend films formed at approximately 700 and 1000 nm, respectively. Therefore, the peak intensity at 700 nm was monitored to determine the amount of polaron formation in the PBDTTPD blend films as a function of the fullerene acceptor, while that at 1000 nm was recorded for the PBDTTT-C films (Figure 6). The TA curves in Figures 6a and c were fitted by a

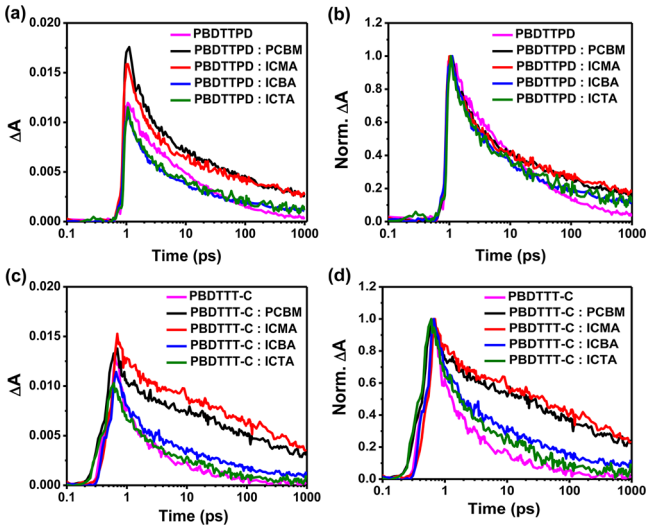

Figure 6. TA curves (a and c) and polaron decay dynamics (b and d) for PBDTTPD and PBDTTT-C, respectively, blended with the PCBM (black), ICMA (red), ICBA (blue), and ICTA (green) films. The pristine polymer films (pink) were measured as controls: (excitation) 610 nm, (excitation fluence) 3 μJ/cm^2.

sum of three exponential functions ($\Delta A = A_1 \exp(-t/\tau_1) + A_2 \exp(-t/\tau_2) + A_3 \exp(-t/\tau_3)$ where ΔA is the TA intensity), which are summarized in Supporting Information Tables S1 and S2. Important parameters are the longest lifetime (τ_3) and its amplitude (A_3), which reflects the long-lived polarons that result from the charge transfer in polymer:fullerene blends.[40,41] All τ_3 and A_3 values of the PBDTTPD and PBDTTT-C blends were compared in Table 4. The polaron yield (A_3) was increased by a factor of almost two for PBDTTPD blended with PCBM and ICMA compared to its blends with ICBA and ICTA, which indicates more efficient charge transfer from donor to acceptor in the PBDTTPD:PCBM (or ICMA) film. In contrast, when a higher fullerene adduct was used instead, the polaron yield reduced dramatically, showing that the polaron yield of

Table 4. Fit Parameters: Amplitude (A_3) and Lifetime (τ_3) for TA Decay of Polarons

	PBDTTPD		PBDTTT-C	
	A_3 (10^{-3})	τ_3 (ps)	A_3 (10^{-3})	τ_3 (ps)
PCBM	4.6	1480	5.0	1629
ICMA	4.5	1520	6.3	1542
ICBA	2.2	1190	1.9	1161
ICTA	2.3	1175	0.9	931
pristine	2.1	390	0.9	289

PBDTTPD:ICBA and PBDTTPD:ICTA was almost the same as the polaron yield of the pristine PBDTTPD polymer. Therefore, the critical value of 0.1 eV for ΔG_{CT} is an important parameter to allow efficient photoinduced charge transfer. Our results were consistent with the results for polyselenophene blended with PCBM reported by Durrant et al., which showed that the polaron yield was strongly dependent on the value of ΔG_{CT}.[42] This correlation between ΔG_{CT} and the polaron yield can also explain the trends of J_{SC} in PBDTTT-C and P3HT-based systems. For example, Figure 6c revealed that the polaron yield of the PBDTTT-C blend films showed a decreasing trend in order of PBDTTT-C:PCBM (ICMA) > PBDTTT-C:ICBA > PBDTTT-C:ICTA films. This trend is similar to that of PBDTTPD blended films. In contrast, the polaron yield in the blend films of P3HT:fullerene bis-adduct was similar to the polaron yield of P3HT:fullerene monoadduct.[28] This result indicated that efficient charge transfer occurs in the P3HT:fullerene bis-adduct film because the value of ΔG_{CT} is still greater than 0.1 eV, unlike the values for the PBDTTPD:ICBA and PBDTTT-C:ICBA films.

Further evidence for the difference in the charge transfer between donor and acceptor as a function of the fullerene acceptor can be provided by the polaron decay dynamics. It was observed that the longest lifetime (τ_3) of the films decreased in the order of PBDTTPD:ICMA (τ_3 = 1520 ps) ~ PBDTTPD: PCBM (τ_3 = 1480 ps) > PBDTTPD:ICBA (τ_3 = 1190 ps) ~ PBDTTPD: ICTA (τ_3 = 1175 ps) > pristine PBDTTPD (τ_3 = 390 ps) films. Similar trend was observed for the τ_3 values of PBDTTT-C blend films, showing the decreasing order of PBDTTT-C:ICMA (τ_3 = 1629 ps) ~ PBDTTT-C:PCBM (τ_3 = 1542 ps) > PBDTTT-C:ICBA (τ_3 = 1161 ps) > PBDTTT-C: ICTA (τ_3 = 931 ps) > pristine PBDTTT-C (τ_3 = 289 ps) films. Thus, the presence of the acceptor material inhibited the recombination of the polarons in the PBDTTPD film due to the charge transfer at the PBDTTPD:fullerene interface, leading to longer polaron lifetimes.[43,44] In addition, the large driving force suppresses the electron back transfer from the acceptor to the polymer; thereby the polaron lifetime of PBDTTPD and PBDTTT-C blended films with PCBM (ICMA) is larger than with fullerene bis- and tris-adducts. Therefore, the lower yield and the shorter lifetime of the polarons in PBDTTPD:ICBA and PBDTTT-C:ICBA indicated reduced efficiency for photoinduced charge transfer, which clearly explains their low EQE and J_{SC} values.

The maximum generation rate (G_{max}) and exciton dissociation probability ($P(E,T)$) were measured to compare PBDTTPD, PBDTTT-C, and P3HT blended with PCBM, ICMA, ICBA, and ICTA. The saturation photocurrent density (J_{sat}), G_{max}, and $P(E,T)$ were calculated using a method in the literature.[27,45] Figure 7 shows the photocurrent densities (J_{ph}) as a function of the effective voltage (V_{eff}) for PBDTTPD, PBDTTT-C, and P3HT blended with PCBM, ICMA, ICBA, and ICTA. Table 5

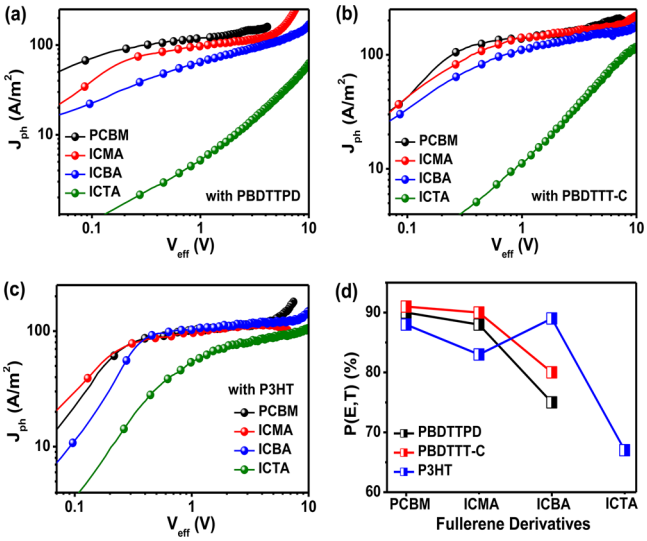

Figure 7. Photocurrent density (J_{ph}) as a function of the effective applied voltage (V_{eff}) for the blend films of (a) PBDTTPD, (b) PBDTTT-C, and (c) P3HT with different fullerene acceptors at optimized conditions. (d) Summary of the $P(E,T)$ values of the blend films.

Table 5. G_{max} and $P(E,T)$ Values for the PBDTTPD, PBDTTT-C, and P3HT Films Blended with Different Fullerenes

blend				
donor	acceptor	J_{sat} [A/m^2]	G_{max} [10^{27} m^{-3} s^{-1}]	$P(E,T)$
PBDTTPD	PCBM	122	7.62	90%
	ICMA	110	6.87	88%
	ICBA	86	5.47	75%
	ICTA			
PBDTTT-C	PCBM	151	9.43	91%
	ICMA	146	9.11	90%
	ICBA	123	7.68	80%
	ICTA			
P3HT	PCBM	113	7.05	88%
	ICMA	106	6.62	83%
	ICBA	115	7.18	89%
	ICTA	80	5.00	67%

summarizes the calculated values of G_{max} and $P(E,T)$ for the blended films.

The G_{max} and $P(E,T)$ of devices made from P3HT blended with PCBM, ICMA, and ICBA had similar values, which agreed with the trend for the J_{SC} values. The $P(E,T)$ values of P3HT:PCBM, P3HT:ICMA, and P3HT:ICBA had similar values of 88%, 83%, and 89%, respectively, which also affects the J_{SC} values of the PSC devices. The G_{max} values of PBDTTPD and PBDTTT-C blended with ICBA were lower than those of their blend films with fullerene monoadduct, i.e., PBDTTPD:ICBA (5.47×10^{27} m^{-3} s^{-1}) vs PBDTTPD:PCBM (7.62×10^{27} m^{-3} s^{-1}) and PBDTTT-C:ICBA (7.68×10^{27} m^{-3} s^{-1}) vs PBDTTT-C:PCBM (9.43×10^{27} m^{-3} s^{-1}). Additional evidence for the reduced charge transfer can be provided from the results in the $P(E,T)$ values. The $P(E,T)$ decreased from 90% (PBDTTPD:PCBM) to 75% (PBDTTPD:ICBA) and from 91% (PBDTTT-C:PCBM) to 80% (PBDTTT-C:ICBA), which was very different from the trend for the P3HT-based PSCs. Interestingly, the $P(E,T)$ values for the PBDTTPD:ICTA and PBDTTT-C:ICTA films cannot be estimated from the J_{ph} vs V_{eff} curves due to the absence of diode characteristics, in contrast to the behavior in the P3HT:ICTA film. The lack of pn-junction characteristics in the PBDTTPD:ICTA and PBDTTT-C:ICTA films provided additional evidence of the inefficient charge transfer and low J_{SC}.

CONCLUSIONS

The photovoltaic behaviors of two different DA copolymers, PBDTTPD and PBDTTT-C, were studied in combination with four different fullerenes, i.e., PCBM, ICMA, ICBA, and ICTA. The results were compared with the behaviors of P3HT-based PSCs. While the P3HT:ICBA devices exhibited higher performance than the P3HT:fullerene monoadduct devices, the PBDTTPD:ICBA and PBDTTT-C:ICBA devices had lower performances than the devices with fullerene monoadducts. We performed PL, EQE, and TA measurements to explore the reasons for the reduced performance of the DA copolymer:ICBA and ICTA blends compared to the blends with the fullerene monoadducts of PCBM and ICMA. The reduction of photoinduced charge transfer in the order of PCBM ~ ICMA > ICBA > ICTA was observed from the EQE and PL measurements. In particular, the EQE values of the PBDTTPD blends with ICBA and ICTA were below 30% and 5%, respectively. The ΔG_{CT} and E_{CT} values explained the loss of J_{SC} and the higher V_{OC} in the PBDTTPD and PBDTTT-C blends with ICBA and ICTA compared to the blends with PCBM and ICMA. To quantify these results, the polaron yield and lifetime at the CT state in the PBDTTPD and PBDTTT-C blends were measured by TA spectroscopy. The polaron yield in PBDTTPD (PBDTTT-C):ICBA was decreased dramatically compared to PBDTTPD (PBDTTT-C):PCBM and PBDTTPD (PBDTTT-C):ICMA due to the insufficient value of ΔG_{CT} i.e., < 0.1 eV. In addition, τ_3 in PBDTTPD:ICBA was shorter than that of the PBDTTPD:fullerene monoadduct. Such a short lifetime of the polaron and insufficient ΔG_{CT} in DA copolymers (PBDTTPD and PBDTTT-C):ICBA would prevent charge transfer from occurring between the polymer and ICBA. Furthermore, the G_{max} and $P(E,T)$ values in the DA copolymer blends decreased when PCBM was replaced by ICBA, whereas the corresponding values in P3HT:PCBM and P3HT:ICBA were similar. Therefore, our observations suggested that optimization of E_{CT} and ΔG_{CT} by controlling the energy level of the fullerene acceptors and polymers while ensuring efficient charge transfer was essential for achieving both high V_{OC} and J_{SC} in BHJ-type PSCs.

ASSOCIATED CONTENT

Supporting Information

Materials and methods, detail experimental procedures, and additional data. This material is available free of charge via the internet at http://pubs.acs.org.

AUTHOR INFORMATION

Corresponding Author

*E-mail: bumjoonkim@kaist.ac.kr.

Notes

The authors declare no competing financial interest.

ACKNOWLEDGMENTS

The authors thank Dr. Claire H. Woo for the helpful discussions. This research was supported by the Korea Research Foundation Grant (2011-0030387, 2011-0010412) and the Seoul R & BD Program (WR090671) funded by the Korean Government. This research was also supported by the New & Renewable Energy

KETEP Grant (2011-3030010060) and the Fundamental R&D Program Grant for Core Technology of Materials funded by the Ministry of Knowledge Economy, Republic of Korea.

REFERENCES

(1) Li, G.; Zhu, R.; Yang, Y. *Nat. Photon.* **2012**, *6*, 153.
(2) Graetzel, M.; Janssen, R. A. J.; Mitzi, D. B.; Sargent, E. H. *Nature* **2012**, *488*, 304.
(3) Scharber, M. C.; Wuhlbacher, D.; Koppe, M.; Denk, P.; Waldauf, C.; Heeger, A. J.; Brabec, C. L. *Adv. Mater.* **2006**, *18*, 789.
(4) He, Z. C.; Zhong, C. M.; Huang, X.; Wong, W. Y.; Wu, H. B.; Chen, L. W.; Su, S. J.; Cao, Y. *Adv. Mater.* **2011**, *23*, 4636.
(5) Green, M. A.; Emery, K.; Hishikawa, Y.; Warta, W.; Dunlop, E. D. *Prog. Photovoltaics* **2012**, *20*, 12.
(6) Boudreault, P. L. T.; Najari, A.; Leclerc, M. *Chem. Mater.* **2011**, *23*, 456.
(7) Chu, T. Y.; Lu, J. P.; Beaupre, S.; Zhang, Y. G.; Pouliot, J. R.; Wakim, S.; Zhou, J. Y.; Leclerc, M.; Li, Z.; Ding, J. F.; Tao, Y. *J. Am. Chem. Soc.* **2011**, *133*, 4250.
(8) Piliego, C.; Holcombe, T. W.; Douglas, J. D.; Woo, C. H.; Beaujuge, P. M.; Frechet, J. M. J. *J. Am. Chem. Soc.* **2010**, *132*, 7595.
(9) Wang, E. G.; Ma, Z. F.; Zhang, Z.; Vandewal, K.; Henriksson, P.; Inganas, O.; Zhang, F. L.; Andersson, M. R. *J. Am. Chem. Soc.* **2011**, *133*, 14244.
(10) Son, H. J.; Wang, W.; Xu, T.; Liang, Y. Y.; Wu, Y. E.; Li, G.; Yu, L. P. *J. Am. Chem. Soc.* **2011**, *133*, 1885.
(11) Huang, Y.; Guo, X.; Liu, F.; Huo, L. J.; Chen, Y. N.; Russell, T. P.; Han, C. C.; Li, Y. F.; Hou, J. H. *Adv. Mater.* **2012**, *24*, 3383.
(12) Miller, N. C.; Sweetnam, S.; Hoke, E. T.; Gysel, R.; Miller, C. E.; Bartelt, J. A.; Xie, X. X.; Toney, M. F.; McGehee, M. D. *Nano Lett.* **2012**, *12*, 1566.
(13) Xin, H.; Subramaniyan, S.; Kwon, T. W.; Shoaee, S.; Durrant, J. R.; Jenekhe, S. A. *Chem. Mater.* **2012**, *24*, 1995.
(14) Cho, C. H.; Kim, H. J.; Kang, H.; Shin, T. J.; Kim, B. J. *J. Mater. Chem.* **2012**, *22*, 14236.
(15) Lenes, M.; Wetzelaer, G. J. A. H.; Kooistra, F. B.; Veenstra, S. C.; Hummelen, J. C.; Blom, P. W. M. *Adv. Mater.* **2008**, *20*, 2116.
(16) Laird, D. W.; Stegamat, R.; Richter, H.; Vejins, V.; Scott, L.; Lada, T. A. *Organic Photovoltaic Devices Comprising Fullerenes and Derivatives Thereof*. Patent application wo 2008/018931 a2., 2008.
(17) He, Y. J.; Chen, H. Y.; Hou, J. H.; Li, Y. F. *J. Am. Chem. Soc.* **2010**, *132*, 5532.
(18) Kang, H.; Cho, C. H.; Cho, H. H.; Kang, T. E.; Kim, H. J.; Kim, K. H.; Yoon, S. C.; Kim, B. J. *ACS Appl. Mater. Interfaces* **2012**, *4*, 110.
(19) Khlyabich, P. P.; Burkhart, B.; Thompson, B. C. *J. Am. Chem. Soc.* **2011**, *133*, 14534.
(20) Guo, X.; Zhang, M.; Huo, L.; Cui, C.; Wu, Y.; Hou, J.; Li, Y. F. *Macromolecules* **2012**, *45*, 6930.
(21) Zhao, G. J.; He, Y. J.; Li, Y. F. *Adv. Mater.* **2010**, *22*, 4355.
(22) Kim, K. H.; Kang, H.; Nam, S. Y.; Jung, J.; Kim, P. S.; Cho, C. H.; Lee, C.; Yoon, S. C.; Kim, B. J. *Chem. Mater.* **2011**, *23*, 5090.
(23) Azimi, H.; Senes, A.; Scharber, M. C.; Hingerl, K.; Brabec, C. J. *Adv. Energy Mater.* **2011**, *1*, 1162.
(24) Faist, M. A.; Kirchartz, T.; Gong, W.; Ashraf, R. S.; McCulloch, I.; de Mello, J. C.; Ekins-Daukes, N. J.; Bradley, D. D. C.; Nelson, J. *J. Am. Chem. Soc.* **2012**, *134*, 685.
(25) Hoke, E. T.; Vandewal, K.; Bartelt, J. A.; Mateker, W. R.; Douglas, J. D.; Noriega, R.; Graham, K. R.; Fréchet, J. M. J.; Salleo, A.; McGehee, M. D. *Adv. Energy Mater* **2012**, DOI: 10.1002/aenm.201200474.
(26) Di Nuzzo, D.; Wetzelaer, G.-J. A. H. W.; Bouwer, R. K. M.; Gevaerts, V. S.; Meskers, C. J. M.; Hummelen, J. C.; Blom, P. W. M.; Janssen, R. A. J. *Adv. Energy Mater* **2012**, DOI: 10.1002/aenm.201200426.
(27) Kim, K. H.; Kang, H.; Kim, H. J.; Kim, P. S.; Yoon, S. C.; Kim, B. J. *Chem. Mater.* **2012**, *24*, 2373.
(28) Faist, M. A.; Keivanidis, P. E.; Foster, S.; Wobkenberg, P. H.; Anthopoulos, T. D.; Bradley, D. D. C.; Durrant, J. R.; Nelson, J. *J. Polym. Sci. Pol. Phys.* **2011**, *49*, 45.
(29) Vandewal, K.; Tvingstedt, K.; Gadisa, A.; Inganas, O.; Manca, J. V. *Phys. Rev. B* **2010**, *81*, 125204.
(30) Vandewal, K.; Tvingstedt, K.; Gadisa, A.; Inganas, O.; Manca, J. V. *Nat. Mater.* **2009**, *8*, 904.
(31) Deibel, C.; Strobel, T.; Dyakonov, V. *Adv. Mater.* **2010**, *22*, 4097.
(32) Zou, Y. P.; Najari, A.; Berrouard, P.; Beaupre, S.; Aich, B. R.; Tao, Y.; Leclerc, M. *J. Am. Chem. Soc.* **2010**, *132*, 5330.
(33) Zhang, Y.; Hau, S. K.; Yip, H. L.; Sun, Y.; Acton, O.; Jen, A. K. Y. *Chem. Mater.* **2010**, *22*, 2696.
(34) Chen, H. Y.; Hou, J. H.; Zhang, S. Q.; Liang, Y. Y.; Yang, G. W.; Yang, Y.; Yu, L. P.; Wu, Y.; Li, G. *Nat. Photon.* **2009**, *3*, 649.
(35) Hou, J. H.; Chen, H. Y.; Zhang, S. Q.; Chen, R. I.; Yang, Y.; Wu, Y.; Li, G. *J. Am. Chem. Soc.* **2009**, *131*, 15586.
(36) Veldman, D.; Meskers, S. C. J.; Janssen, R. A. J. *Adv. Funct. Mater.* **2009**, *19*, 1939.
(37) Bredas, J. L.; Norton, J. E.; Cornil, J.; Coropceanu, V. *Acc. Chem. Res.* **2009**, *42*, 1691.
(38) Cho, H. H.; Kang, T. E.; Kim, K. H; Kang, H.; Kim, H. J; Kim, B. J. *Macromolecules* **2012**, *45*, 6415.
(39) Pommerehne, J.; Vestweber, H.; Guss, W.; Mahrt, R. F.; Bassler, H.; Porsch, M.; Daub, J. *Adv. Mater.* **1995**, *7*, 551.
(40) Hwang, I. W.; Xu, Q. H.; Soci, C.; Chen, B. Q.; Jen, A. K. Y.; Moses, D.; Heeger, A. J. *Adv. Funct. Mater.* **2007**, *17*, 563.
(41) Meng, K.; Ding, Q.; Wang, S. F.; He, Y. J.; Li, Y. F.; Gong, Q. H. *J. Phys. Chem. B* **2010**, *114*, 2602.
(42) Clarke, T. M.; Ballantyne, A. M.; Tierney, S.; Heeney, M.; Duffy, W.; McCulloch, I.; Nelson, J.; Durrant, J. R. *J. Phys. Chem. C* **2010**, *114*, 8068.
(43) Tong, M. H.; Coates, N. E.; Moses, D.; Heeger, A. J.; Beaupre, S.; Leclerc, M. *Phys. Rev. B* **2010**, *81*, 125210.
(44) Muller, J. G.; Lupton, J. M.; Feldmann, J.; Lemmer, U.; Scharber, M. C.; Sariciftci, N. S.; Brabec, C. J.; Scherf, U. *Phys. Rev. B* **2005**, *72*, 195208.
(45) Wu, J. L.; Chen, F. C.; Hsiao, Y. S.; Chien, F. C.; Chen, P. L.; Kuo, C. H.; Huang, M. H.; Hsu, C. S. *ACS Nano* **2011**, *5*, 959.